DEUTSCHES ELEKTRONEN-SYNCHROTRON DESY

DESY SR 84-24
October 1984

KINETICS OF EXCITED STATES PRODUCED BY SYNCHROTRON RADIATION

by

G. Zimmerer
II. Institut für Experimentalphysik, Hamburg, Germany

ISSN 0723-7979

NOTKESTRASSE 85 · 2 HAMBURG 52

To be sure that your preprints are promptly included in the
HIGH ENERGY PHYSICS INDEX ,
send them to the following address (if possible by air mail) :

DESY
Bibliothek
Notkestrasse 85
2 Hamburg 52
Germany

DESY SR 84-24
October 1984

ISSN 0723-7979

KINETICS OF EXCITED STATES PRODUCED BY SYNCHROTRON RADIATION

G. ZIMMERER

II. Institut für Experimentalphysik, Luruper Chaussee 149, D-2000 Hamburg 50, (Fed. Rep. Germany)

ABSTRACT

This paper describes, how synchrotron radiation can be used as an excitation source in time- and spectrally resolved fluorescence in connection with experiments on the kinetics of electronically excited atoms or molecules. As examples, the formation and the decay of various excimer systems are discussed. In addition, a few aspects of intramolecular dynamics in diatomic molecules are sketched.

INTRODUCTION

Since many years, synchrotron radiation (SR) is used for excitation purposes in molecular dynamics experiments. The unique properties of the source make feasible nearly δ-like vibrationally and in the case of small molecules even rotationally resolved selective excitation in the vacuum ultraviolet (VUV) spectral range. This is the basis for various kinds of experiments to exploit in detail dynamical processes in molecular physics. Fragmentation, ionization, dissociation, relaxation, intersystem crossing, and elementary chemical reactions were already investigated. A comprehensive review on the early papers (up to 1978) was given by Koch and Sonntag (ref.1).

Of special importance in probing dynamical processes is fluorescence spectroscopy. The pioneering efforts in time- and spectrally resolved fluorescence under state selective excitation with SR were undertaken at ACO (ref.2), at SPEAR (ref.3), and at DESY (ref.4). In the meantime, a unique experimental station (SUPERLUMI) for such measurements was constructed in the Hamburger Synchrotronstrahlungslabor HASYLAB at DESY (ref.5,6). Part of the results presented in this paper, were obtained with this apparatus.

After a short description of the set-up and the experimental techniques used, the formation and the decay of excimer molecules like rare gas dimers (R_2), rare gas halides, and rare gas hydrides are discussed. The last part will cover some aspects of Rydberg-valence interaction of excited states in diatomic molecules.

to be published in "Photophysics and Photochemistry above 6 eV", ed. by P. Rigny, Elsevier Science Publishers B.V., Amsterdam

Properties of the source

The properties of SR were already described in detail elsewhere (ref.7,8). In short we can summarize:

(i) SR has a continuous spectral distribution extending from the infrared (IR) to the x-ray region.

(ii) SR (from a storage ring) has a unique time structure. It consists of light pulses with a fwhm between 1 ns and .1 ns. The repetition frequency ranges between 1 MHz and 500 MHz.

(iii) SR is laserlike collimated (vertically).

(iv) SR has a well defined polarization.

The set-up SUPERLUMI

In this set-up, 50 mrad (horizontal) of SR are collected and spectrally dispersed by a 2m-normal incidence (NI) monochromator (ref.5). The flux obtained with this optical layout is comparable to what is obtained with more recent wiggler sources (ref.9).

TABLE 1

Technical parameters of the experimental set-up SUPERLUMI.

Excitation	resolution interval	working range	flux/f-number
2m-NI monochromator	$\delta\lambda \geq .007$ nm	30 - 330 nm	2×10^{12} phot./sec*
Analysis			
.5m asymmetric Pouey mounting	$\delta\lambda \geq .5$ nm	50 - 300 nm	f/2.8
.5m double monochromator, mod. Czerny-Turner-mounting	$\delta\lambda \geq .03$ nm	200 -1000 nm	f/5
Detectors	**time resolution****		**quantum efficiency*****
windowless channel plate, CsJ-sensitized	$\geq$ 50 ps	$\leq$ 180 nm	10 %
solar blind type with MgF_2 window (Hamamatsu R1460)	$\geq$ 5 ns	120 - 300 nm	15 %
Valvo XP2020Q	$\geq$100 ps	160 - 550 nm	25 %
RCA C31034	$\geq$100 ps	200 - 930 nm	13 %

* This number holds for $\delta\lambda$ = 1 nm at a beamcurrent of 100 mA for a grating covered with Al + MgF_2 in the blaze maximum.

** The lower limit of lifetimes which can be measured is given here. In all cases, an upper limit is 10 µs.

*** Estimates for the maximum.

The monochromatic light is focused inside the ultra-high vacuum (UHV) sample

chamber which can be equipped with a gas cell, a He-cryostat etc. Fluorescence is analysed at right angle to the exciting beam with two monochromators. One of them covers the VUV spectral range and has an extremely large acceptance (f/2.8) at a medium resolution (ref.6). The other one extends the wavelength range to the near IR.

In connection with the time structure of the storage ring DORIS (fwhm=130 ps; rep. rate $\geq$ 1 MHz), time constants τ between 50 ps and 10 μs can be measured. Relevant numbers characterizing the set-up are given in Table 1.

Besides conventional absorption- and reflection spectroscopy, *stationary fluorescence* and *fluorescence excitation spectra* (fluorescence intensity as a function of excitation wavelength, λ_{ex}) can be measured. For time-resolved spectroscopy, the single-photon and timing method (delayed coincidences) (ref.4,10) is used. With this method, with fixed λ_{ex} and λ_{an} (fluorescence wavelength), *rise- and decay curves* can be measured. In *time-resolved fluorescence spectra* (λ_{ex} fixed), the fluorescence intensity is measured within a time window δt (> .5 ns) at a fixed delay ΔT ($0 \leq \Delta T \leq 1$ μs) as a function of λ_{an}. In *time-resolved excitation spectra*, the fluorescence intensity is registrated within δt, however, as a function of λ_{ex} (λ_{an} being fixed).

FORMATION, DECAY AND POTENTIAL CURVES OF EXCIMERS

Introduction

In the last years, excimers attracted much interest because many of them are used as laser molecules in UV and VUV gas lasers (ref.11). Neglecting the small thermodynamic concentration of dimers in, e.g., dense rare gases, excimers are generally formed in reactive collisions of electronically excited atoms or molecules with ground state species. It was amply demonstrated, that SR can be used as an excitation source to study the kinetics of such excimer systems. After initial experiments on rare gas dimers, R_2 (R: Xe, Kr, Ar) the investigations were extended to rare gas monohalides. Very recently, rare gas halides were included because of the particular interest in these simplest rare gas compounds.

Rare gas dimers

Kinetics. Schematic potential curves are given in Fig. 1. The 0_g^+ ground state is repulsive apart from a shallow Van der Waals minimum at large internuclear distance. Correlating with $^3P_1$ and $^3P_2$ excited atoms, bound excited states (0_u^+ and $1_u/0_u^-$) exist. Details of the potential curves are given, e.g., in ref.12 (Xe_2), ref.13 (Kr_2), and ref.14 (Ar_2). R_2 molecules are identified by their characteristic bound-free fluorescence. At high pressure, the vibrationally relaxed molecules emit the so-called "second continuum", whereas at low pressure, the decay of vibrationally excited molecules dominates ("first

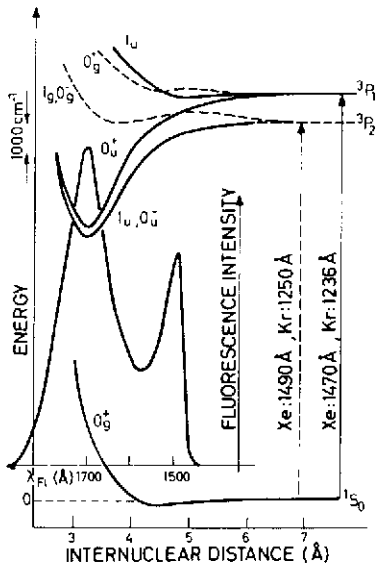

Fig. 1. Potential curves and fluorescence spectrum of a rare gas dimer.

continuum") (ref.15). In Fig. 1, a typical fluorescence spectrum of Xe_2 is included with the second continuum at ~ 170 nm and the first continuum at ~ 148 nm (intermediate pressure). The emission of the 0_u^+ and 1_u state spectrally overlap. They can be separated in time-resolved experiments.

The complex kinetics even under primary state selective excitation could be disentangled making use of the tunability of the SR source (ref.16). Fig. 2 shows, e.g., the temporal behaviour of the second continuum of Xe_2 for different pressures and excitation wavelengths. Excitation from the ground state to 0_u^+ and 1_u well below the $^3P_2$ atomic level leads to a simple temporal behaviour. The decay curves display both the 0_u^+ (fast) and 1_u (slow) emission. From the pressure dependence, the radiative lifetimes of the states involved, average vibrational relaxation rates, and the rate constants for collisional mixing of 0_u^+ and $1_u/0_u^-$ were extracted for Kr_2 and Xe_2 (ref.16-18). As an example, in Fig. 3 the pressure dependence of the Xe_2 $1_u/0_u^-$ lifetime is shown (lowest part).

Excitation of Xe_2 or Kr_2 in the vicinity of $^3P_2$ leads to collisional dis-

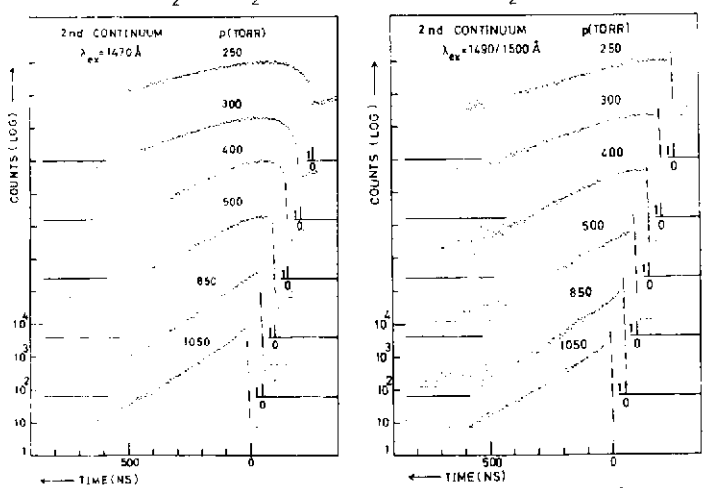

Fig. 2. Decay curves of the second continuum of Xe_2^* for different λ_{ex} and various pressures.

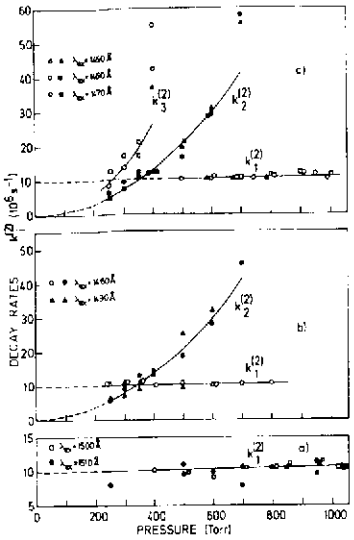

Fig. 3. Decay rates of the second continuum of Xe_2^* for various λ_{ex} as a function of gas pressure.

sociation into $^3P_2$ atoms (ref.16) which then act as reservoir from which the molecules are formed predominantly by three-body collisions,

$$R^*(^3P_2) + 2R \rightarrow R_2^*(1_u/0_u^-) + R \qquad (1)$$

The temporal behaviour of the second continuum is of the cascade-type and displays the actual lifetime of the precursor (= $k_2^{(2)}$ in fig. 3 with its strong p^2-contribution) and the lifetime of the $1_u/0_u^-$ state. With further increasing excitation energy, the atomic $^3P_1$ state is populated. As a relaxation scheme, we now have to take into account (simplified)

$$R^*(^3P_1) \overset{2R}{\rightarrow} R_2^*(0_u^+, \text{high } v') \overset{R}{\rightarrow} R^*(^3P_2) \overset{2R}{\rightarrow}$$
$$R_2^*(1_u/0_u^-, \text{high } v') \overset{R}{\rightarrow} R_2^*(1_u/0_u^-, \text{low } v') \qquad (2)$$

In the decay curves the lifetimes of both reserviors and the lifetimes of the emitting states show up. Numerical results are given in Table 2.

TABLE 2

Comparison of the lifetimes of Kr_2^* and Xe_2^* excimer states and of the two-body rate constants of formation measured with SR excitation. Lifetimes are given in ns, rate constants in $cm^6 s^{-1}$.

Radiative lifetimes			reaction	rate constant	
$Kr_2^*(0_u^+)$	3.4	a)	$Kr^*(^3P_1)+2Kr \rightarrow Kr_2^*(0_u^+)+Kr$	3.2×10^{-32}	a)
	5.2	b,c)		1 x "	b)
$Kr_2^*(1_u/0_u^-)$	264	a)		5.1x "	c)
	245	c)	$Kr_2^*(^3P_2)+2Kr \rightarrow Kr_2^*(1_u/0_u^-)+Kr$	1.78x "	b)
				1.97x "	c)
				2.2x "	d)
$Xe_2^*(0_u^+,\text{high } v')$	2.5	b)	$Xe^*(^3P_1)+2Xe \rightarrow Xe_2^*(0_u^+)+Xe$	5x "	b,h)
	1.6	e)		5.3x "	f)
$Xe_2^*(0_u^+,\text{low } v')$	4.6	f)		3.4x "	d)
	6.9	g)			
$Xe_2^*(1_u/0_u^-)$	101	b,h)	$Xe^*(^3P_2)+2Xe \rightarrow Xe_2^*(1_u/0_u^-))+Xe$	7.5x "	b,h)
	99	f)			
	112	g)			
	105	e)			
	45-60	i)			

a)ref.18 b)ref.19 c)ref.20 d)ref.15 e)ref.21 f)ref.22 g)ref.17
h)ref.16 i)ref.23

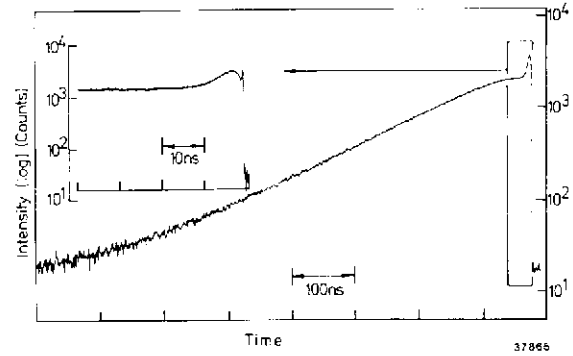

Fig. 4. Decay curve of the second continuum of Kr_2^* at 800 torr. In the insert, the number of channels/ns is 40 x higher than in the other curve.

The decay curves of Fig. 2 were measured with a solar blind type detector (BX 762). The tremendous progress realized with channel plate detectors is demonstrated in Fig. 4. It shows a decay curve of Kr_2^* excited with λ_{ex} = 124,8 nm (ref.24). This is an excitation near to the crossing of the 0_u^+ and the $1_g/0_g^-$ state (Fig. 1). The wavelength of analysis was 147 nm (center of the second continuum). At this wavelength, not only the emission of vibrationally relaxed, but also of vibrationally excited molecules is observed. The tiny spike (insert) stems from the initially excited molecules which collisionally dissociate into $^3P_2$ atoms or relax vibrationally. Those molecules which relax within the 0_u^+ state, emit the second fast peak (insert) with a risetime (= vibrational relaxation) and a decay (= lifetime of the 0_u^+ state). The slow contribution stems from those molecules which were formed in the 1_u state via the atomic $^3P_2$ reservoir.

Determination of potential curves. The potential curves of the excited states (0_u^+, $1_u/0_u^-$) are only known at large internuclear distances (from absorption measurements) and around their minima (from high pressure fluorescence) (see, e.g., ref.12-14). At small internuclear distances, experimental determinations are scarce. In principle, the potential curves can be extracted from the bound-free fluorescence spectra of molecules excited selectively at high v' (Fig. 5). However, in order to have a considerable concentration of R_2 ground state molecules which then can be excited selectively, a high particle density is required which then destroys the initial vibrational population by collisions. Dutuit et al. (ref.25) overcame this problem for the first time by measuring the fluorescence within a time window δt (Fig. 5) immediately following pulsed excitation with SR at ACO. In the case of Xe_2, they measured the long wavelength onset of fluorescence (which stems from the "inner turning point") and extracted the 0_u^+ potential curve.

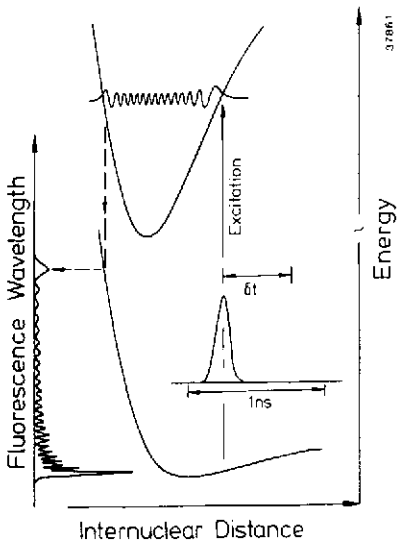

Fig. 5. Schematic explanation of the oscillatory structure of emission from the "inner turning point".

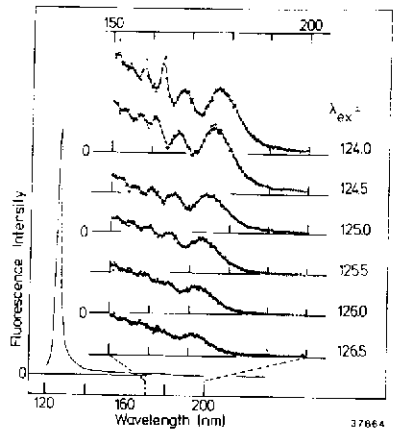

Fig. 6. First continuum of Kr_2^* for various λ_{ex}. Time window 8 ns. Pressure 10^{3} torr.

With the new set-up SUPERLUMI it was possible to resolve the oscillatory structure of the bound-free fluorescence spectra emitted at short internuclear distances for Xe_2, Kr_2, and Ar_2. The long wavelength onset is correlated to λ_{ex} in the expected way (smaller λ_{ex} leads to a red shift of the onset). As an example, in Fig. 6 Kr_2 results are shown (ref.24,26). The oscillations and the onset are visible only in a considerably magnified scale (insert). In connection with recent high resolution laser excitation studies (ref.27) the extraction of reliable potential curves of the ground state and of the excited state should be possible in the near future.

Rare gas monohalides

Some remarks on the kinetics of formation. The efficiency of SR as a tunable and pulsed excitation source was demonstrated recently in a study of the formation and the decay of rare gas monohalides in R/Cl_2 mixtures (R: Xe, Kr, Ar). Using SR at ACO, it was shown that the monohalides are not only formed in reactions of the typ

$$R^* + Cl_2 \rightarrow (RCl)^* + Cl \qquad (3)$$

but also following primary electronic excitation of Cl_2 itself:

$$R + Cl_2^* \rightarrow (RCl)^* + Cl \qquad (4)$$

This follows from, e.g., the excitation spectra of the monohalide B → X emission (XeCl: 308 nm, KrCl: 222 nm, ArCl: 175 nm) in R/Cl_2 mixtures

(ref.28,29). The experiments were continued at HASYLAB (ref.30,31).

As an example, Ar/Cl_2 is discussed. In this system, two competing fluorescence channels, the Cl_2 $2^3\Pi_g$ emission at 258 nm and the ArCl B → X emission itself are observed. Fig. 7 shows the excitation spectra of both bands (ref.30). In the transparency range of Ar (λ_{ex} > 107 nm) they exhibit rich structures, some of them being assigned to the $1\,^1\Sigma_u^+$, the $2\,^1\Sigma_u$ and the $2\,^1\Pi_u$ state of Cl_2 (ref.32). It is obvious that ArCl can only be formed under primary excitation with λ_{ex} < 130 nm (this threshold is ascribed to the *energetic* threshold of the reaction and leads to formation of ArCl in the minimum of the B-state (ref.30).

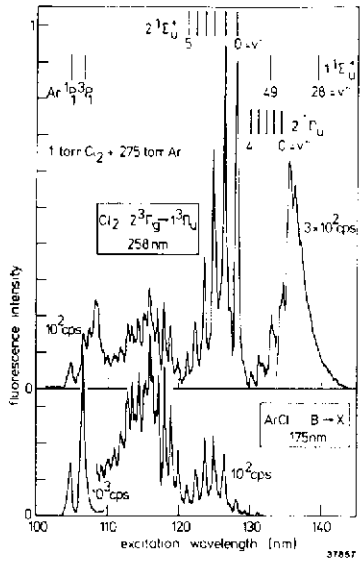

Fig. 7. Excitation spectra of Cl_2 $2^3\Pi_g$ and ArCl B → X emission in Cl_2 doped Ar.

Decay of rare gas monohalides and B/C mixing. The decay of the B → X emission of rare gas monohalides is of great interest for laser application. Therefore, the decay was studied in a wide range of rare gas pressure (~ 2 torr to ~ 1000 torr) following selective excitation of the Cl_2 precursor in R/Cl_2 mixtures. Details, including numerical values for the rate constants of various processes involved, are given in another contribution in this volume (ref.36). Only one example is presented here which underlines once more the efficiency of the excitation source.

As already mentioned, ArCl can be produced at the bottom of the B-state, if Cl_2 is excited in the $2\,^1\Sigma_u^+$ v' = 0 state (however, $2\,^1\Sigma_u^+$ is not the electronic state involved in the elementary reaction, see below). Then, the decay rate of B → X emission is described by (Fig. 8)

$$K = \frac{1}{\tau_B} + k_1(Cl_2)\, p_{Cl_2} + k_1(Ar)\, p_{Ar} + k_2(Ar)\, p_{Ar}^2 \qquad (5)$$

B/C mixing can be neglected. Reliable two- and three-body rate constants and the radiative lifetime of the B state (v' = 0) were extracted (ref.30,36).

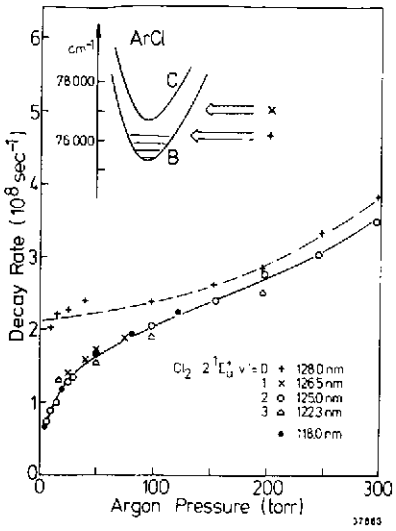

Fig. 8. Decay rate of ArCl B → X emission as a function of Ar pressure for various excitation wavelengths.

Tuning the primary excitation to v' $\geq$ 1 of the $2^1\Sigma_u^+$ state of Cl_2 dramatically changes the situation. In the elementary reaction, both B- and C-state molecules are created. B/C mixing by collisions takes place. Then the B → X emission contains two rates. The slower one approaches the parabolic behaviour only at high p_{Ar}. At lower p_{Ar} it yields a deflection and then goes down to an intercept which corresponds to the lifetime of the C state at p_{Ar} = 0 (Fig. 8). The deflection is typical for the slower decaying state (here the C state) being above the faster one (ref.36). Whereas in the case of XeCl and KrCl the B → X decay is correctly described in the whole pressure range by a two-level model for B/C mixing, this is not the case for ArCl. Here the B/C energy separation is much larger than the vibrational quantum ($\Delta E(B-C) \approx 5 \times \hbar\omega_o$) (ref.30,36). The mixing is better described in a "two-ladder" model of the vibrational levels of the B and the C state (ref.37).

Rare gas hydrides

This class of excimers attracted much interest from point of view of theory (ref.38). A safe experimental proof of the existence was up to now not achieved except for ArH (ref.39). The reason is obvious from the insert of Fig. 9. It shows calculated potential curves of the ground state and the lowest excited states (HeH, ref.40). The potential curves are very close one to each other at short internuclear distances. If the hydrides are formed in high vibrational levels of the excited states, many of them obviously predissociate into the ground state and the characteristic fluorescence is quenched.

The tunability of the SR excitation source comes into play here again. For the first time, Möller proved, that hydrides are formed in collisions of the type

$$R + H_2^* \rightarrow (RH)^* + H \qquad (6)$$

if H_2 is excited into it's C state (ref.41). The hydrides are monitored by

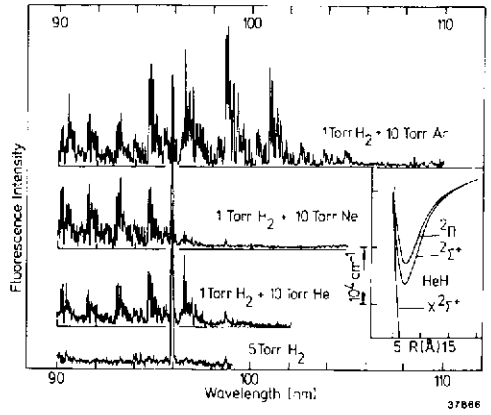

Fig. 9. Excitation spectra of rare gas hydride fluorescence in H_2 doped He, Ne, Ar. The structures are rotationally resolved bands of the $H_2C^1\Pi_u$ state (v' = 0: 100.89 nm, v' = 1: 98.59 nm, v' = 2: 96.55 nm, v' = 4: 92.98 nm, etc.). Details see text.

their radiative decay in the visible and near UV (190 nm - 500 nm; $B^2\Pi \rightarrow X^2\Sigma^+$ transition; ref.41). Fig. 9 shows excitation spectra of HeH, NeH, and ArH emission. In all cases, a threshold of formation is observed with a systematic trend. The threshold of formation is ascribed to the *energetical* threshold of the elementary reaction, which was deduced from the calculated minima of the excited states of the hydrides and the binding energy of H_2 (ref.41)

For comparison, in Fig. 9 an excitation spectrum of light eventually emitted by pure H_2 into the same spectral range as covered by hydride emission is included. Within the sensitivity of the set-up, no H_2 emission is observed (the lines at 95.8 nm and 98.6 nm stem from traces of N_2).

The experiment of Möller is pioneering also from another point of view. The gas cell used was equipped with an In window* because the excitation wavelengths used were below the LiF cut-off. Pressures up to 50 torr were used. This clearly demonstrates that - due to the high sensitivity of SUPERLUMI - the excitation wavelength in time- and spectrally resolved fluorescence experiments on dense gases is no longer limited to $\lambda_{ex} > 104$ nm (LiF cut-off).

RYDBERG-VALENCE INTERACTION IN DIATOMIC MOLECULES

Introduction

In the preceding part, some aspects of *intermolecular* dynamics were discussed. We now go on with a specific aspect of *intramolecular* dynamics. In many molecules, avoided crossing phenomena between diabatic states of the same symmetry lead to splittings and adiabatic double-well potential curves as is shown in Fig. 10 for Cl_2. By far not all potential curves are given. The references for the curves are given in ref.32. The cases discussed here, are avoided crossings of Rydberg- and valence-type states.

* The high quality In windows were produced by Mr. H. ZEIGER in the preparation laboratory of HASYLAB.

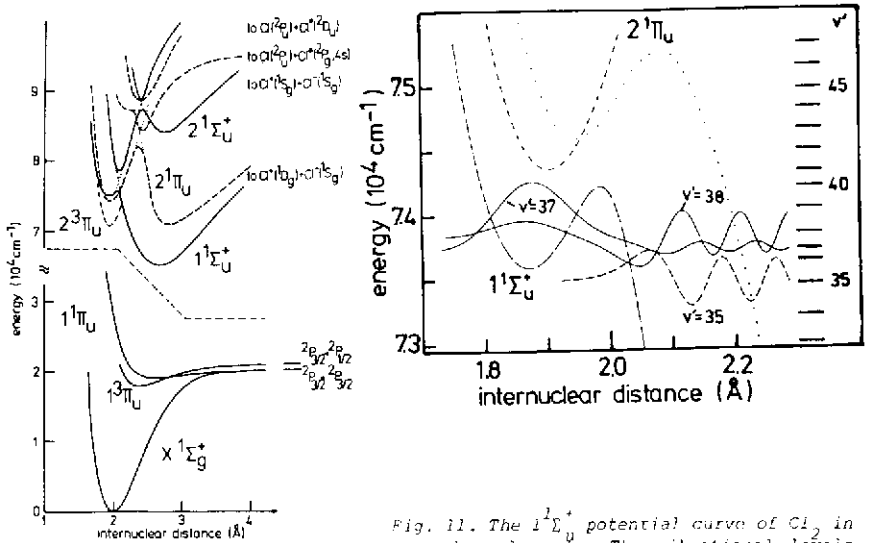

Fig. 10. Potential curves of Cl_2 with various avoided crossings (not complete, see text).

Fig. 11. The $1^1\Sigma_u^+$ potential curve of Cl_2 in an enlarged scale. The vibrational levels and selected wavefunctions of $1^1\Sigma_u^+$ are included. The dotted curve is a calculation (ref.43).

The purpose of this chapter is to show, how a combination of absorption and fluorescence spectroscopy with SR excitation can help to deduce double-well potential curves and information about the diabatic crossing of the gap between both adiabatic states involved.

Cl_2

In spite of many efforts, even in high resolution spectroscopy experiments (ref.42), an unambiguous assignment of the various progressions in the VUV was not possible, because Rydberg-valence interaction effects lead to very irregular vibrational sequences. Using SR excitation and combining absorption and fluorescence spectroscopy, the regular $2^1\Pi_u$, the 0_u^+ and 1_u components of $2^3\Pi_u$, the double-well $1^1\Sigma_u^+$ and the $2^1\Sigma_u^+$ state, which stem from an avoided crossing, were analysed in detail (ref.32). The inner-well region of the $1^1\Sigma_u^+$ potential curve is shown in an enlarged scale (ref.32) in Fig. 11 (together with $2^1\Pi_u$; the dotted curve was calculated (ref.43)). Please, note the irregular spacing of the vibrational levels of $1^1\Sigma_u^+$.

The adiabatic wavefunctions v' = 37 and 38 are of particular interest. Under selective excitation, due to the large amplitude in the inner-well region, pronounced bound-bound $1^1\Sigma_u^+ \rightarrow X\ ^1\Sigma_g^+$ fluorescence is observed from the v' = 37 level, which is nearly absent, if v' = 38 is excited (Fig. 12, ref.32). The long wavelength parts of the spectra in Fig. 12 stem from the outer well and

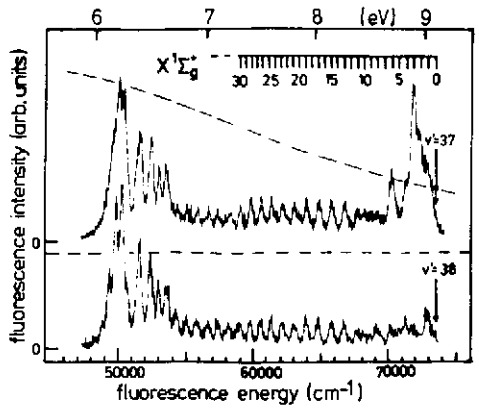

Fig. 12. Fluorescence of Cl_2 following primary excitation of v' = 37 (upper curve) and v' = 38 of the $1^1\Sigma_u^+$ state. Dashed curve: transmission characteristics of the set-up.

contain both a $1^1\Sigma_u^+ \rightarrow X\ ^1\Sigma_g^+$ bound-bound and a bound-free contribution with its pronounced maximum at ~ 200 nm corresponding to the transition at the maximum of the difference potential (ref.44).

Fluorescence experiments of this kind were important to assign certain features in absorption which did not fit into a regular progression. Another puzzle was solved in this way. Whereas most of the bands of $1^1\Sigma_u^+$ are red-shaded (outer-well region), especially v' = 37 is blue shaded (ref.32), a fact which prevented an assignment to the same electronic state before (ref.32,42).

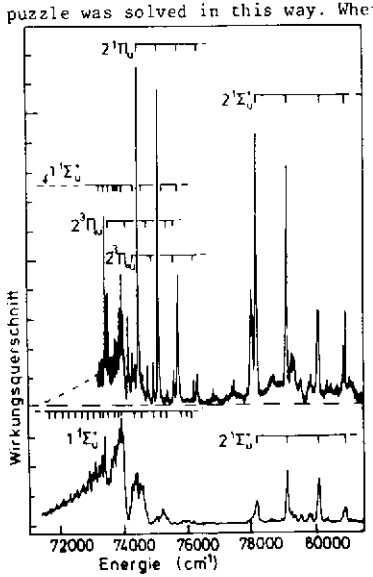

Fig. 13. Absorption cross section (upper curve) and fluorescence excitation spectrum of Cl_2 (ref.44,45).

The key for the deduction of the $1^1\Sigma_u^+$ state was the fluorescence excitation spectrum. In Fig. 13 (ref.44,45), the excitation spectrum of the integrated fluorescence (which contains practically only $1^1\Sigma_u^+$ emission) is compared with the absorption cross section. The most dominant absorption features ($1^1\Pi_u$, $2^3\Pi_{0_u^+,1_u}$) do not show up in the excitation spectrum. It was concluded that the excitation spectrum is a measure of the cross section of $1^1\Sigma_u^+$ (ref.32).

The $2^1\Sigma_u^+$ state leads to $1^1\Sigma_u^+$ emission (excitation above 78000 cm^{-1}). However, the amplitudes of the absorption cross-sections and the excitation spectrum are different (Fig. 13). The fluorescence yield is

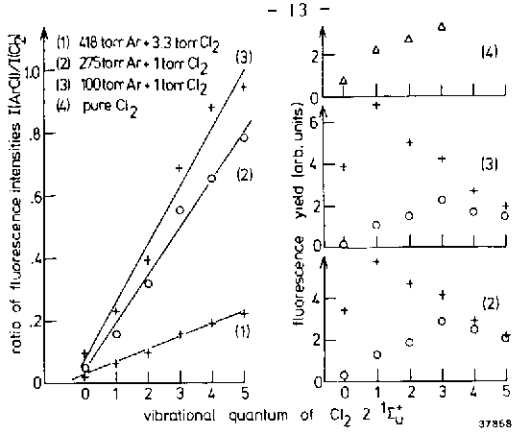

Fig. 14. Fluorescence yield of Cl_2 ($1^1\Sigma_u^+$) (Δ) in pure Cl_2, and of Cl_2^* ($2^3\Pi_g$) (+) and ArCl (B → X) (o) in Ar/Cl_2 mixtures as a function of v' of $2^1\Sigma_u^+$ (right part).

plotted as a function of v' of $2^1\Sigma_u^+$ in Fig. 14 (upper right part). Möller et al. (ref.44,45) tentatively correlated the behaviour of the fluorescence yield to the Landau-Zener probabilities of diabatic crossing of the gap between $2^1\Sigma_u^+$ and $1^1\Sigma_u^+$ (Fig. 10). Whether this interpretation is valid with respect to a complete analysis of the perturbation is an interesting question for theory.

The latter result is interesting from another point of view. In Fig. 14, below the fluorescence yield in pure Cl_2, the yield of the Cl_2^* ($2^3\Pi_g$) emission and the yield of ArCl* (B → X) emission in Cl_2 doped Ar is given (ref.30). The composition of the mixtures (2) and (3) is given in the left part. The yield of ArCl* (B → X) emission is ~ proportional to the yield of $1^1\Sigma_u^+$ emission in pure Cl_2. From this result it was concluded, that - even under primary excitation of $2^1\Sigma_u^+$ - the precursor in the reaction Cl_2^* + Ar → ArCl* + Cl is the $1^1\Sigma_u^+$ state (ref.30).

HCl

The insert of Fig. 15 shows selected calculated potential curves of this molecule (ref.46). It is obvious that similar effects must occur than in Cl_2. From the first absorption and fluorescence measurements which were performed with SR excitation, it turns out that the situation may even be more complicated (ref.47). Because the work under discussion is still in progress, only one result is presented here, which is also interesting from an experimental point of view.

The fluorescence of the $2^1\Sigma^+$ state can be clearly separated in an inner-well and an outer-well part. The inner-well part contains a long wavelength $2^1\Sigma^+$

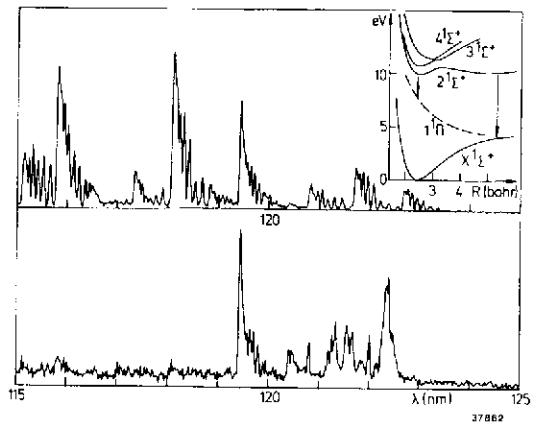

Fig. 15. Excitation spectra of $2^1\Sigma^+$ emission of $H^{35}Cl$ (ref.47). Upper curve: transition corresponding to the right arrow, lower curve: - left arrow in the insert which presents calculated potential curves of HCl (ref.46).

→ $1^1\Pi$ contribution, whereas the outer-well part decays only into the ground state at shorter wavelengths. Fig. 15 shows excitation spectra of the two decay channels indicated by arrows in the insert. The rotational substructure of the different vibrational transitions is clearly observed (isotope-clean $H^{35}Cl$ was used). Both spectra are drastically different. From this result we expect that the interaction of the diabatic states can be studied rotationally resolved. This will be of particular importance, if lifetimes are studied under rotational selective excitation.

ACKNOWLEDGEMENTS

A great part of the work was carried out together with Drs. M.C. Castex and J. LeCalvé (Paris) and Dr. D. Haaks (Wuppertal). This fruitful collaboration is gratefully acknowledged. I am especially obliged to my co-workers in Hamburg for their enthusiasm and continuous efforts. Among them I want to mention Dipl. Phys. T. Möller and cand. phys. M. Beland and J. Stapelfeld who agreed to present unpublished results of their thesis/Diploma works. The work of Dipl. Phys. E. Roick and Dr. P. Gürtler who built up SUPERLUMI, and the efforts of the group of Prof. N. Schwentner (Berlin) in constructing the high intensity beamline, are gratefully acknowledged.

The work was supported by the BMFT of the Federal Republic of Germany.

REFERENCES

1 E.E. Koch and B. Sonntag, in C. Kunz (Ed.), Synchrotron Radiation, Springer, Berlin, Heidelberg, New York, 1979, pp. 267-355
2 L. Lindquist, R. Lopez-Delgado, M.M. Martin and A. Tramer, in G.V. Marr and I.H. Munro (Eds.), Proceedings of the Internat. Symp. for Synchrotron Radiation Users, Daresbury, U.K., D.N.P.L./R28, 1973, pp. 257-266
M. Lavollée and R. Lopez-Delgado, Rev. Sci. Instrum., 48 (1977) 816-821
3 K.M. Monahan and V. Rehn, Nucl. Instr. and Methods, 152 (1978) 255-259
4 R. Brodmann, R. Haensel, U. Hahn, U. Nielsen and G. Zimmerer, Chem. Phys. Letters, 29 (1974) 250-252
U. Hahn, N. Schwentner and G. Zimmerer, Nucl. Instr. and Methods, 152 (1978) 261-264
5 H. Wilcke, W. Böhmer, R. Haensel and N. Schwentner, Nucl. Instr. and Methods, 208 (1983) 59-63
6 P. Gürtler, E. Roick, G. Zimmerer and M. Pouey, Nucl. Instr. and Methods, 208 (1983) 835-839
7 C. Kunz (Ed.), Synchrotron Radiation, Springer, Berlin, 1979
8 D.E. Eastman and Y. Farge (General Eds.), Handbook on Synchrotron Radiation, North-Holland, Amsterdam, vol. 1A and 1B, 1983
9 P. Gürtler and A. Jackson, Nucl. Instr. and Methods, 208 (1983) 163-166
10 I.H. Munro and N. Schwentner, Nucl. Instr. and Methods, 208 (1983) 819-834
11 Ch.K. Rhodes (Ed.), Excimer Lasers, Topics in Appl. Physics, vol. 30, Springer, Berlin, 1979
12 M.C. Castex, J. Chem. Phys., 74 (1981) 759-771
13 F.X. Gadea, F. Spiegelmann, M.C. Castex and M. Morlais, J. Chem. Phys., 78 (1983) 7270-7283
14 M.C. Castex, M. Morlais, F. Spiegelmann and J.P. Malrieu, J. Chem. Phys., 75 (1981) 5006-5016
15 R. Brodmann and G. Zimmerer, J. Phys. B: Atom. Molec. Phys., 10 (1977) 3395-3408
16 H.D. Wenck, S.S. Hasnain, M.M. Nikitin, K. Sommer, G. Zimmerer and D. Haaks, Chem. Phys. Lett., 66 (1979) 138-143
17 G. Thornton, E.D. Poliakoff, E. Matthias, S.H. Southworth, R.A. Rosenberg, H.C. White and D.A. Shirley, J. Chem. Phys., 71 (1979) 133-139
18 T.D. Bonifield, F.H.K. Rambow, G.K. Walters, M.V. McCusker, D.C. Lorents and R.A. Gutchek, Chem. Phys. Lett., 69 (1980) 290-296
19 H.D. Wenck, M.C. Castex, D. Haaks, M.M. Nikitin, B. Jordan and G. Zimmerer, in Extended Abstracts of the VIth Internat. Conf. VUV Rad. Phys. Charlottesville, Virginia, U.S.A., June 2-6, 1980, III-9 (3 p.)
20 U. Rieck, Diplomarbeit, University of Hamburg (1983)
21 E.D. Poliakoff, M.G. White, S.-T. Lee, R.A. Rosenberg, E. Matthias and D.A. Shirley, in M.C. Castex, M. Pouey and N. Pouey (Eds.), Extended Abstracts of the Vth Internat. Conf on VUV Rad. Phys., Montpellier, France, Sept. 5-9, 1977, I-64
22 T.D. Bonifield, F.H.K. Rambow, G.K. Walters, M.V. McCusker, D.C. Lorents and R.A. Gutchek, J. Chem. Phys., 72 (1980) 2914-2924
23 M. Ghelfenstein, H. Szwarc and R. López-Delagado, Chem. Phys. Lett., 52 (1977) 236-238
24 T. Möller, M. Beland, J. Stapelfeldt and G. Zimmerer, to be published
25 O. Dutuit, M.C. Castex, J. LeCalvé and M. Lavollée, J. Chem. Phys., 73 (1980) 3107-3113
26 T. Möller, thesis, University of Hamburg (in progress)
27 R.H. Lipson, P.E. LaRocque and B.P. Stoicheff, Optics Lett., 9 (1984) 402-404
28 M.C. Castex, J. LeCalvé, D. Haaks, B. Jordan and G. Zimmerer, Chem. Phys. Lett., 70 (1980) 106-111
29 J. LeCalvé, M.C. Castex, D. Haaks, B. Jordan and G. Zimmerer, Il Nuovo Cimento, 63B (1981) 265-275

30 B. Jordan, T. Möller, G. Zimmerer, D. Haaks, J. LeCalvé and M.C. Castex, to be published
31 B. Jordan, thesis, University of Hamburg (1983)
32 T. Möller, B. Jordan, P. Gürtler, G. Zimmerer, D. Haaks, J. LeCalvé and M.C. Castex, Chem. Phys., 76 (1983) 295-306
33 E.D. Poliakoff, S.H. Southworth, M.G. White, G. Thornton, R.A. Rosenberg and D.A. Shirley, J. Chem. Phys. 72, (1980) 1786-1792
34 K.M. Monahan, V.O. Jones and V. Rehn, J. Chem. Phys., 71 (1979) 2360-2365
35 K.Y. Tang and D.C. Lorents, in Proc. Internat. Conf. on Lasers, New Orleans, CA, U.S.A., Dec. 15-19, 1980, STS Press, McLean VA, U.S.A., 1981, p. 692-698
36 J. LeCalvé, M.C. Castex, D. Haaks, B. Jordan, T. Möller and G. Zimmerer, this volume
37 D. Haaks, private communication
38 G. Theodorakopoulos, S.C. Farantos, R.J. Buenker and S.D. Peyerimhoff, J. Phys. B: At. Mol. Phys., 17 (1984) 1453-1462, and references therein
39 J.W.C. Johns, J. Molec. Spectrosc., 36 (1970) 488-510
40 B. Rosen, Spectroscopic Data Relative to Diatomic Molecules, Pergamon Press, Oxford, 1970, p. 442, and references therein
41 T. Möller, to be published
42 A.E. Douglas, Can. J. Phys., 59 (1981) 835-840
43 S.D. Peyerimhoff and R.J. Buenker, Chem. Phys., 57 (1981) 279-296
44 T. Möller, Diplomarbeit, University of Hamburg, 1982, and Interner Bericht DESY F 41 - HASYLAB 82-07, Oct. 1982
45 T. Möller, J. LeCalvé, M.C. Castex, D. Haaks, B. Jordan, P. Gürtler and G. Zimmerer, Annals of the Israel Phys. Soc., 6 (1983) 374-376
46 M. Bettendorff, S.D. Peyerimhoff and R.J. Buenker, Chem. Phys., 66 (1982) 261-279
47 M. Beland, J. LeCalvé, M.C. Castex, D. Haaks, T. Möller and G. Zimmerer, in progress